

Boundedness Issues in Planning of Locomotion Trajectories for Biped Robots

Leonardo Lanari, Seth Hutchinson and Luca Marchionni

Abstract—It is in general complex to consider the complete robot dynamics when planning trajectories for bipedal locomotion. We present an approach to trajectory planning, with the classical Linear Inverted Pendulum Model (LIPM), that takes explicit consideration of the unstable dynamics. We derive a relationship between initial state and the control input that ensures the overall system dynamics will converge to a stable steady state solution. This allows us to exploit the unstable dynamics to achieve system goals, while imposing constraints on certain degrees of freedom of the input and initial conditions. Based on this, we propose an approach to trajectory planning, and derive solutions for several typical applications. Experimental simulations using the REEM-C biped robot platform of Pal Robotics validate our approach.

I. INTRODUCTION

In this paper, we address the problem of planning locomotion trajectories for bipedal robots. Our approach begins by using the classical Linear Inverted Pendulum Model (LIPM) to approximate the robot dynamics. Although the LIPM is unstable (e.g., [1]), for any specific input there exist initial conditions from which the system will converge to a stable steady state solution. Likewise, for any initial conditions, there exists a stabilizing input. In this paper, we derive a constraint – the boundedness constraint – that relates the LIPM initial conditions to its input, such that the system dynamics converge to a stable steady state when the constraint is satisfied. We then apply this constraint to derive control strategies that will achieve various locomotion goals, such as resisting external disturbances, arriving to a desired state at a specified time, etc. Finally, we use these control strategies as input to a full dynamic simulation of the REEM-C biped robot to demonstrate their effectiveness. Our results argue that it is feasible to derive control strategies for humanoid robot locomotion by considering explicitly the unstable dynamics of the LIPM approximation in order to derive, for example, zero moment point (ZMP) trajectories.

The remainder of the paper is organized as follows. In Section II we provide a brief review of related research. Since the LIPM is by now well known in the bipedal locomotion community, in Section III we give only a high level overview of model and its application to bipedal locomotion. In Section IV we derive a constraint on initial conditions and input that ensures boundedness of the unstable dynamics

of the LIPM. We then extend this analysis to characterize trajectories of the stable dynamics, and finally of the center of mass (CoM) dynamics. In Section V, we show how the analysis of Section IV can be used to solve trajectory planning problems for locomotion, as well as how to solve directly for state trajectories by setting up appropriate boundary value problems. In Section VI, we give several specific application problems to demonstrate our approach, including deriving inputs to achieve desired terminal conditions and resisting external disturbance. In Section VII, we present full dynamic simulations of the PAL Robotics humanoid REEM-C robot. Finally, in Section VIII we describe the relationship between our approach and several existing methods.

II. RELATED RESEARCH

For more than two decades, the LIPM has been widely used to approximate the dynamics of bipedal robots for gait planning [1]. Under this approximation, the relationship between the ZMP and the center of mass (CoM) is governed by an unstable second order system. One of the more successful approaches using this approximation is the Preview Control based approach of Kajita [2]. It is assumed that the planner knows the future reference trajectory for a finite horizon thus leading to a non-causal control approach. The approach illustrated in Section IV also contains a non-causal aspect.

In the work of Harada and colleagues [3]–[6], trajectory planning has been formulated as a two-point boundary value problem (TPBVP) that is solved analytically for a family of polynomial ZMP trajectories allowing real-time implementation. A combination of these techniques is used in [4] where the TPBVP approach is used for a nominal part while Preview Control is applied on the perturbation dynamics. A clear presentation of the problems related to these approaches can be found in [7]. Some of these aspects have been addressed in [8] by allowing higher order polynomials and expanding the concept of simultaneous planning of CoM and ZMP trajectories. The work in [9] gives a thorough treatment of boundary conditions and their connection to gait planning problems. In [10] and [7], the LIPM is extended using a three-mass system, taking into account the trajectory of the swinging leg. A closely related point of view is presented in [11] using Model Predictive Control. A Fourier series based approximate solution is given in [12] where an additional smoothing is also required.

Also related to our approach is the research done on capture point dynamics, since these coincide with the unstable mode of the LIPM. The seminal paper of Pratt et al. [13] introduced the *capture point* as the point on the

S. Hutchinson is Professor of Electrical and Computer Engineering at the University of Illinois. E-mail: seth@illinois.edu. L. Lanari is with the Dipartimento di Ingegneria Informatica, Automatica e Gestionale, Sapienza Università di Roma, Via Ariosto 25, 00185 Rome, Italy. E-mail: lanari@diag.uniroma1.it. L. Marchionni, is a Robotics Engineer with Pal Robotics, Pujades 77-79, 08005 Barcelona, Spain. E-mail: luca.marchionni@pal-robotics.com

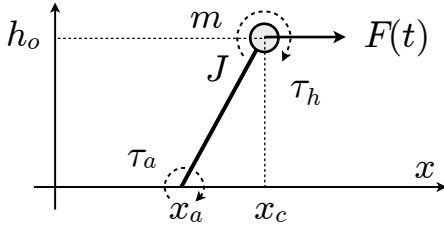


Fig. 1. The Linear Inverted Pendulum (LIPM)

ground where the humanoid had to step in order to come to a complete stop after the push has vanished. The analysis carried on the LIPM was enriched with the use of an ankle torque or a flywheel to maintain balance before a step was needed. A complementary result defining decision surfaces was presented in [14]. The introduction of the Foot Point Estimation [15] where a nonlinear model of a rimless wheel with only two spokes was used, allowed the inclusion of the energy loss due to the ground impact. Reactive stepping strategies are developed in [16] by considering the capture point and the neutral point in a TPBVP framework. The capture point concept has been used successfully also for walking gaits in [17]. We refer to the complete bibliography of [18] for a complete overview.

III. THE LINEAR INVERTED PENDULUM

Researchers often resort to approximate models of the dynamics during trajectory planning, and then rely on closed-loop control schemes to stabilize the actual robot during locomotion. As described above, the LIPM is a popular approximation that has proven to be effective for this purpose.

The LIPM dynamics [2], [18] in the sagittal plane are

$$\ddot{x}_c = \frac{g}{z_o}(x_c - x_a) + \frac{1}{mh_o}(\tau_a - \tau_h) + \frac{F(t)}{m} \quad (1)$$

with, see Fig. 1, x_a the point foot location, x_c the CoM x -position, h_o its constant height, m its concentrated mass, τ_a an ankle torque and τ_h a hip torque acting on a reaction mass. The explicit contribution of a possibly time-varying disturbance force $F(t)$ acting in the x -direction is also included. The equations for the lateral component of motion are similar, so we do not include these here.

Defining $\omega_o = \sqrt{g/h_o}$, we may rewrite (1) as

$$\ddot{x}_c(t) = \omega_o^2 x_c(t) - \omega_o^2 z(t) \quad (2)$$

in which $z(t)$ accounts for all external inputs to the dynamic equations for the CoM, including possible disturbance.

As shown in [18], model (2) can be instantiated to represent basic gait models and is therefore general enough to encompass a wide variety of dynamic models for locomotion.

- *Point foot.* With no torques present the pendulum is represented as a massless telescoping leg with point foot location in x_a and a point mass m kept at a constant height h_o . The Center of Pressure (CoP) is fixed in x_a if no step is taken. In this case x_a can be considered as a control input, and in the absence of external disturbances we have

$$\ddot{x}_c = \omega_o^2 x_c - \omega_o^2 x_a \quad (3)$$

- *Finite-sized foot.* If we allow a finite-sized foot with an ankle torque τ_a , the CoP location can be changed by the ankle torque since $x_{cop} = x_a - \tau_a/(mg)$ and therefore (1) can be rewritten as

$$\ddot{x}_c = \omega_o^2 x_c - \omega_o^2 x_{cop} \quad (4)$$

For flat foot contact on a horizontal surface the CoP coincides with the Zero Moment Point [19] (ZMP) i.e. $x_{cop} = x_{zmp}$. In this context, the CoP is used as a control input.

- *Reaction mass.* In order to mimic human behavior in balancing, arm and torso movements can, at least approximately, be represented by an actuated reaction mass which generates a momentum around the CoM and therefore an acceleration along the x -axis. We omit the rotational dynamics of the reaction mass since it is not essential in our framework. Defining the Centroidal Moment Pivot (CMP) as

$$x_{cmp} = x_{cop} + \frac{\tau_h}{mg} = x_a - \frac{\tau_a - \tau_h}{mg} \quad (5)$$

we obtain the system dynamics

$$\ddot{x}_c = \omega_o^2 x_c - \omega_o^2 x_{cmp} \quad (6)$$

In the sequel, we use (2) as the LIPM dynamic model, since equations (3), (4) and (6) are variations of this equation.

IV. BOUNDED SOLUTIONS FOR THE LIPM MODEL

In this section, we first review the state space description of the LIPM dynamics, and use the change of coordinates of [7] that decouples its unstable and stable modes. Then, in Section IV-B we provide the first main result of the paper — a constraint on the initial conditions and input that ensures boundedness of the unstable subsystem trajectories. In Section IV-C, we give a kind of dual analysis for the stable system. Then, in Section IV-D we relate the results from Sections IV-B and IV-C to the CoM trajectory. A point-mass robot taking a single step is used to illustrate the concepts. More interesting cases are given in Section VI.

A. LIPM equivalent state-space representations

System (2) can be represented in the CoM position and velocity (x_c, \dot{x}_c) coordinates and with input $z(t)$ by

$$S_c : \begin{pmatrix} x_c \\ \dot{x}_c \end{pmatrix} \quad A_c = \begin{pmatrix} 0 & 1 \\ \omega_o^2 & 0 \end{pmatrix} \quad B_c = \begin{pmatrix} 0 \\ -\omega_o^2 \end{pmatrix}$$

Applying the change of coordinates

$$\begin{pmatrix} x_u \\ x_s \end{pmatrix} = \begin{pmatrix} 1 & 1/\omega_o \\ 1 & -1/\omega_o \end{pmatrix} \begin{pmatrix} x_c \\ \dot{x}_c \end{pmatrix} \quad (7)$$

we can fully decouple the stable and unstable dynamics

$$\dot{x}_u = \omega_o x_u - \omega_o z \quad (8)$$

$$\dot{x}_s = -\omega_o x_s + \omega_o z \quad (9)$$

Note that the unstable dynamics x_u coincide with the capture point dynamics [18], also named divergent component of motion [7], [17] or extrapolated center of mass [20].

We desire to select trajectories of the system that remain bounded and avoid the divergent behavior associated to the

eigenvalue $+\omega_o$. This can be accomplished either by an appropriate choice of initial condition $x_u(t_0)$, or by designing the input $z(t)$ to maintain $x_u(t)$ bounded¹. To this end, we will analyze the two subsystems, x_u and x_s , separately in Sections IV-B and IV-C, which will allow us to relate constraints on the inputs and the initial conditions to performance goals (e.g., center of mass position and velocity at the final time). By taking this approach, the stable dynamics can be viewed as allowing extra degrees of freedom for the control design.

B. Unstable subsystem

The solution of (8) for general input $z(t)$ is given by

$$x_u(t; z) = e^{\omega_o(t-t_0)}x_u(t_0) - \omega_o \int_{t_0}^t e^{\omega_o(t-\tau)}z(\tau)d\tau \quad (10)$$

Note that we use the notation $x_u(\cdot; z)$ to make explicit the dependence on choice of control input z . In general, this solution diverges; however, as shown in [21], [22], if the initial condition satisfies

$$x_u(t_0) = x_u^*(t_0; z) \triangleq \omega_o \int_{t_0}^{\infty} e^{-\omega_o(\tau-t_0)}z(\tau)d\tau \quad (11)$$

we obtain the particular solution

$$x_u^*(t; z) = \omega_o \int_0^{\infty} e^{-\omega_o\tau}z(\tau+t)d\tau \quad (12)$$

which is bounded under mild boundedness conditions on the input $z(t)$. Here, we use the notation $x_u^*(\cdot; z)$ to denote the particular trajectory of the system under the input z when the initial condition on x_u satisfies (11). This solution depends on the future values of the input z , and therefore is anticausal. Although this may sound odd, it has already been noticed in [2] that the CoM trajectory must be noncausal with respect to the desired ZMP trajectory.

Consider, for example, as input $z = z_{\text{step}}(t-t_a)$, with $z_{\text{step}}(\cdot)$ the Heaviside step function. Then (11) and (12) become

$$\begin{aligned} x_u^*(0; z) &= \omega_o \int_0^{\infty} e^{-\omega(\tau+t_a)}d\tau = e^{-\omega_o t_a} \\ x_u^*(t; z) &= e^{\omega_o(t-t_a)}[z_{\text{step}}(t) - z_{\text{step}}(t-t_a)] + z_{\text{step}}(t-t_a) \end{aligned} \quad (13)$$

Fig. 2 illustrates the trajectory of x_u for this case.

Under the change of coordinates given by (7), the condition (11) also implies a constraint on the initial conditions for the center of mass trajectory, namely

$$x_u^*(t_0; z) = x_u(t_0) = x_c(t_0) + \frac{1}{\omega_o}\dot{x}_c(t_0) \quad (14)$$

In the sequel, we refer to (14) as the *boundedness condition*.

¹Note that the term ‘‘bounded’’ here is referred to the given input, i.e. we want to avoid the divergence due to the unstable eigenvalue ω_o and obtain a behavior similar to the concept of steady-state. For example, if the input were a ramp we could admit a similar behavior even if it is diverging.

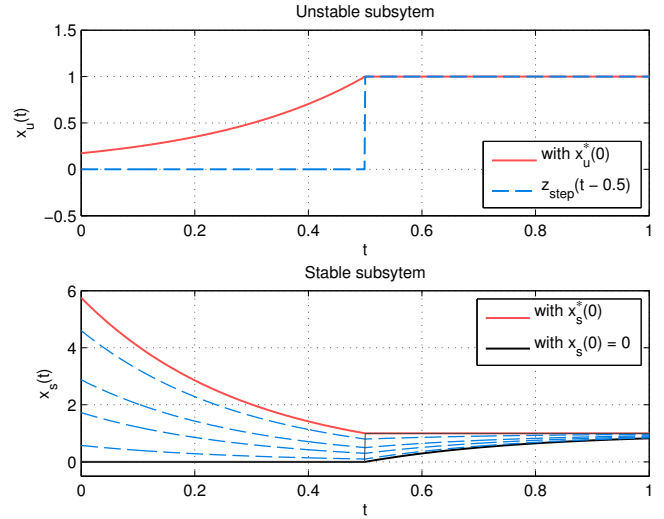


Fig. 2. Effect of $x_u^*(0; z)$ on the unstable system trajectory - Trajectories $x_s(t)$ for various initial conditions of the form $x_s(0) = kx_s^*(0; z)$ for $k = 1, 0.8, 0.5, 0.3, 0.1, 0$.

C. Stable Subsystem

Let us now consider the stable subsystem given by (9). Since this system is stable, for any initial condition $x_s(t_0)$, the trajectory $x_s(t)$ will asymptotically converge to a steady-state solution if it exists. However, if the input $z(t)$ is equal to 0 for all $t < t_a$ and is defined as $z(t) = v(t-t_a)z_{\text{step}}(t-t_a)$, then, for any $t_0 < t_a$, it may be possible to select the initial condition $x_s(t_0)$ such that $x_s(t)$ evolves as its steady-state solution from time t_a on (i.e., the steady-state solution is achieved at the moment the input is applied). This particular initial condition is defined as

$$x_s(t_0) = x_s^*(t_0; z) \triangleq \omega_o e^{\omega_o(t_a-t_0)} \int_{-\infty}^{t_a} e^{\omega_o(\tau-t_a)}v(\tau)d\tau \quad (15)$$

Consider again the example illustrated in Fig. 2 in which $z = z_{\text{step}}(t-t_a)$, with $t_0 = 0$. In this case, (15) becomes

$$x_s^*(0; u) = \omega_o \int_{-\infty}^{t_a} e^{\omega_o\tau}d\tau = e^{\omega_o t_a} \quad (16)$$

and therefore

$$x_s^*(t; z) = e^{-\omega_o(t-t_a)}[z_{\text{step}}(t) - z_{\text{step}}(t-t_a)] + z_{\text{step}}(t-t_a)$$

denotes the particular trajectory starting in t_0 that will lead to the steady-state behavior from t_a on.

Fig. 2 illustrates various trajectories for x_s for different choices of initial condition. In particular, the red trajectory corresponds to $x_s(0) = x_s^*(0; z)$ and the black trajectory corresponds to $x_s(0) = 0$. Other trajectories shown correspond to $x_s(0) = kx_s^*(0; z)$

D. CoM trajectory

Under the change of coordinates given by (7), the center of mass trajectory corresponding to x_u^* and x_s^* is given by

$$x_c^* = \frac{1}{2}(x_u^* + x_s^*) \quad \dot{x}_c^* = \frac{\omega_o}{2}(x_u^* - x_s^*)$$

When the initial state of the stable subsystem deviates from $x_s^*(0, z)$, a full range of CoM behaviors is possible. In this case, we can write the trajectory $x_c(t)$ directly in terms of this deviation as

$$\begin{aligned}
x_c &= \frac{1}{2}(x_u^* + x_s) \\
&= \frac{1}{2}(x_u^* + e^{-\omega_o t} x_s(0) + \omega_o \int_0^t e^{-\omega_o(t-\tau)} z(\tau) d\tau) \\
&= \frac{1}{2}(x_u^* + e^{-\omega_o t} (x_s(0) - x_s^*(0; z)) \\
&\quad + e^{-\omega_o t} x_s^*(0; z) + \omega_o \int_0^t e^{-\omega_o(t-\tau)} z(\tau) d\tau) \\
&= \frac{1}{2}(x_u^* + e^{-\omega_o t} (x_s(0) - x_s^*(0; z)) + x_s^*(t)) \\
&= x_c^* + \frac{1}{2} e^{-\omega_o t} (x_s(0) - x_s^*(0; z)) \tag{17}
\end{aligned}$$

Note that (17) gives a complete characterization of all bounded solutions parameterized by the initial condition $x_s(0)$. Furthermore, note that x_c asymptotically approaches x_c^* for any initial condition $x_s(0)$. This implies that if the boundedness condition (14) is satisfied, $x_c \rightarrow x_c^*$.

This asymptotic behavior of any x_c belonging to the considered family of bounded solutions, with an abuse of notation, may allow us to define x_c^* as the steady state behavior of the system under the effect of the input $z(t)$.

Consider again the example given above with $z = z_{\text{step}}(t - t_a)$, and $x_u^*(t)$, $x_s^*(t)$ previously computed. In this case, the resulting center of mass trajectory is given by

$$\begin{aligned}
x_c^*(t) &= \cosh(\omega_o(t - t_a)) [z_{\text{step}}(t) - z_{\text{step}}(t - t_a)] \\
&\quad + z_{\text{step}}(t - t_a) \\
\dot{x}_c^*(t) &= \omega_o \sinh(\omega_o(t - t_a)) [z_{\text{step}}(t) - z_{\text{step}}(t - t_a)]
\end{aligned}$$

For this case, Fig. 3 shows the CoM trajectories given by (17) for a range of values of $x_s(0)$, including $x_s(0) = x_s^*(0, u)$ (in red) and $x_s(0) = 0$ (in black).

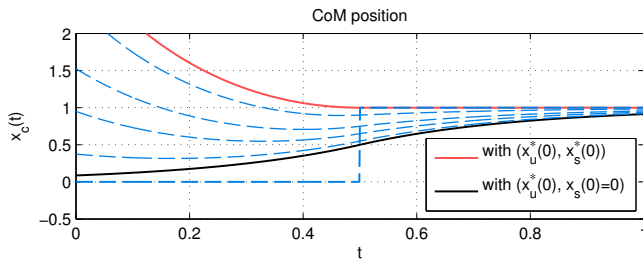


Fig. 3. CoM trajectory $x_c(t)$ for $x_u(0) = x_u^*(0; z)$, and differing choices for $x_s(0)$.

V. PLANNING AND CONTROL DESIGN

As described above in Section IV, condition (14) is necessary to ensure a bounded solution for the CoM trajectory. Since (14) depends on both the initial conditions of the system and on the input, it can be used either to infer constraints on the initial conditions when the input is

specified, or to derive constraints on the design of $z(t)$ in the case where the initial conditions are specified. In this section, we discuss each of these cases. Following this, in Section VI we present solutions for a few specific problems.

A. Constraints on Initial Conditions

If the input $z(t)$ is known (for example if a desired ZMP trajectory is given, or in the case of a known external disturbance), then we can directly evaluate $x_u^*(t_0; z)$ using (11), and (14) then defines a linear constraint between $x_c(t_0)$ and $\dot{x}_c(t_0)$. For example, if $x_c(t_0)$ is specified, we have

$$\dot{x}_c(t_0) = \omega_o [x_u^*(t_0; z) - x_c(t_0)]$$

In this case, we have a boundary value problem in which the boundary conditions are

$$x_c(t_0) = \text{Actual initial CoM position}$$

$$x_u^*(t_0; u) = \text{Bounded unstable solution selection}$$

If, on the other hand, $\dot{x}_c(t_0)$ is given, we have the explicit constraint on CoM initial position

$$x_c(t_0) = x_u^*(t_0; z) - \frac{1}{\omega_o} \dot{x}_c(t_0)$$

leading to a boundary value problem in which the boundary conditions are

$$\dot{x}_c(t_0) = \text{Actual initial CoM velocity}$$

$$x_u^*(t_0; z) = \text{Bounded unstable solution selection}$$

Finally, note that in the case when the input $z(t)$ is known for all $t \geq t_0$, (14) can be viewed as an extension of the classical capture point condition. In particular, in the unforced case (i.e. for $z = 0$), we have $x_u^*(t_0; 0) = 0$, leading to $x_c(t_0) = -\dot{x}_c(t_0)/\omega_o$, which is the classical capture point condition. When $z \neq 0$, (14) generalizes the notion of capture point to give the initial condition from which the unstable subsystem will converge for the input z .

B. Constraints on Control Design

Alternatively, if the initial conditions on the center of mass trajectory are given, (14) can be viewed as a constraint on the design of the control input $z(t)$. In particular, consider the case in which the system input is a linear combination of a disturbance input, z_{dist} , and a control input, z_{cont} , with z_{cont} chosen as a linear combination of known functions z_i

$$z_{\text{cont}} = \sum \alpha_i z_i(t) \tag{18}$$

For example, the z_i could be a collection of step functions, cubic splines or the monotonic functions used in [9]. For this class of inputs, we can rewrite (14) to infer constraints on the choice of the design parameters α_i

$$\begin{aligned}
x_u(t_0) &= x_u^*(t_0; z) \\
&= x_u^*(t_0; z_{\text{cont}}) + x_u^*(t_0; z_{\text{dist}}) \tag{19}
\end{aligned}$$

$$= \sum_i \alpha_i x_u^*(t_0; z_i) + x_u^*(t_0; z_{\text{dist}}) \tag{20}$$

where (19) and (20) follow due to the linearity of (11) in $z(t)$. Note that in (20) each expression $x_u^*(t_0; z_i)$ and $x_u^*(t_0; z_{\text{dist}})$ can be directly evaluated using (11), since z_i and z_{dist} are known functions. Therefore, (20), defines a linear constraint on the α_i . Given a sufficient number of other constraints (e.g., initial or final conditions for CoM trajectory, smoothness constraints at individual steps, etc.), we may solve uniquely for the α_i . On the other hand, if there are not enough constraints to uniquely determine the α_i , we could choose to optimize various performance criteria using the extra degrees of freedom.

VI. APPLICATIONS

For illustration purposes, we consider the point foot case so that control inputs of the form $z_i = z_{\text{step}}(t - t_i)$ also represent physical footsteps by the robot. Recall from (13) that in this case, $x_u^*(0; z_i) = e^{-\omega_o t_i}$.

A. Single Footstep for Arbitrary CoM Initial Conditions

Consider the case for which the robot will take a single step at time t_1 , i.e., $z(t) = z_{\text{step}}(t - t_1)$. In this case, combining (20) and (14) we obtain

$$\alpha x_u^*(0; z_{\text{step}}(t - t_1)) = \alpha e^{-\omega_o t_1} = x_c(0) + \frac{1}{\omega_o} \dot{x}_c(0) \quad (21)$$

$$\alpha = e^{\omega_o t_1} \left(x_c(0) + \frac{1}{\omega_o} \dot{x}_c(0) \right) \quad (22)$$

Thus, for any initial CoM position $x_c(0)$ and velocity $\dot{x}_c(0)$, we are able to obtain a bounded trajectory by choice of the magnitude of a single step. Furthermore, we have $(x_c, \dot{x}_c) \rightarrow (x_c^*, \dot{x}_c^*)$ and $(x_c^*, \dot{x}_c^*) \rightarrow (1, 0)$. This solution is closely related to the well-known capture point condition for selecting a single footstep that will bring the robot to rest from its initial conditions. In particular, the quantity inside the parentheses corresponds to the capture point, and the magnitude of the step is determined by both the capture point, and the amount of time that passes before executing the step.

B. Disturbances

For illustration purposes we now show how the design approach can help in determining the proper steps when the humanoid is disturbed by some known force $F(t)$. For example a known change in the terrain slope can be modeled as a constant known force acting on the CoM

$$F(t) = F z_{\text{step}}(t - T) \quad \text{or} \quad z_{\text{dist}}(t) = \frac{1}{m\omega_o^2} F(t) \quad (23)$$

where T is the instant at which we want the swinging foot to touch the ground with the new known slope. The disturbance enters the CoM equation according to (1). In order to plan this transition step properly starting from the actual initial CoM conditions (position and velocity) we need the new

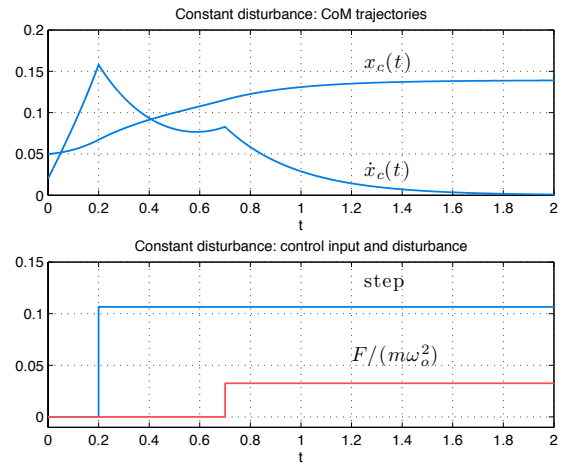


Fig. 4. Constant disturbance anticipative compensation from a generic CoM initial condition, $t_a = 0.2$ sec, $T = 0.7$ sec

step $x_a = \alpha_a z_{\text{step}}(t - t_a)$, with $t_a \leq T$, in order to make the boundedness condition (20) satisfied, that is

$$\begin{aligned} x_u(0) &= \frac{F}{m\omega_o^2} x_u^*(0; z_{\text{step}}(t - T)) + \alpha_a x_u^*(0; z_{\text{step}}(t - t_a)) \\ &= \frac{F}{m\omega_o^2} e^{-\omega_o T} + \alpha_a e^{-\omega_o t_a} \end{aligned}$$

which, solving in the step length α_a , leads to

$$\alpha_a = e^{\omega_o t_a} \left(x_c(0) + \frac{\dot{x}_c(0)}{\omega_o} \right) - \frac{F}{m\omega_o^2} e^{\omega_o(t_a - T)} \quad (24)$$

In this example, the anticipative effect of our design, when possible, is evident and illustrated in Fig. 4. The step is taken in advance knowing the disturbance will act later. Moreover note that the final CoM configuration has a CoM position value which differs from the value of the step length α_a and this means the LIPM is not perpendicular wrt to the ground. This difference arises since the humanoid needs to compensate the effect of the constant disturbance z_{dist} .

C. Steady state control

An interesting situation arises when we succeed in imposing both constraints (14) and (15) that is

$$\begin{aligned} x_u(0) &= x_u^*(0; z) && \text{Boundedness Constraint} \\ x_s(0) &= x_s^*(0; z) && \text{Steady State Constraint} \end{aligned}$$

with $z(t) = v(t - t_a) z_{\text{step}}(t - t_a)$. Constraint (14) guarantees that a bounded x_u^* exists, while (15) makes x_s exactly follow the steady state from t_a on or, equivalently, x_c follow x_c^* from t_a on. This particular situation is similar to the concept of deadbeat. We can therefore guarantee that, at the time the last input is applied, the humanoid has definitively reached a final configuration and remains there. Referring for illustration purposes to the disturbance example shown in Fig. 4 of Section (VI-B) where the CoM position reaches it's final value asymptotically, adding a second step $\alpha_b z_{\text{step}}(t - t_b)$

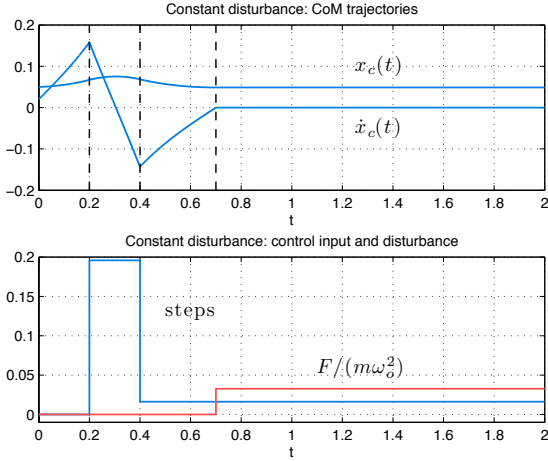


Fig. 5. Constant disturbance with steady state design $t_a = 0.2$ sec, $t_b = 0.4$ sec, $T = 0.7$ sec

and the steady state constraint (15)

$$\begin{aligned}
 x_s(0) &= x_c(0) - \frac{\dot{x}_c(0)}{\omega_o} \\
 &= x_s^*(0; z_{\text{dist}}(t)) + \alpha_a x_s^*(0; z_{\text{step}}(t - t_a)) \\
 &\quad + \alpha_b x_s^*(0; z_{\text{step}}(t - t_b)) \\
 &= \frac{F}{m\omega_o^2} e^{\omega_o T} + \alpha_a e^{\omega_o t_a} + \alpha_b e^{\omega_o t_b}
 \end{aligned}$$

leads to the behavior shown in Fig. 5 where the final constant CoM position is reached at T with the relative position w.r.t. the final step position remaining the same as in Fig. 4.

D. Other useful design conditions

From the previous analysis it is clear that as long as we can express a design constraint linearly w.r.t. the design parameters α_i , the resulting equations will be easier to solve. We could for example require that the total distance covered by the gait should be equal to a given distance d_{des} . Since we have chosen to illustrate these concepts with simple point foot steps $z_i = z_{\text{step}}(t - t_i)$, the total distance will just be

$$d_{\text{des}} = \sum \alpha_i \quad (25)$$

and therefore the condition is easily stated.

We can also design our steps amplitude in order to make the CoM be at some specific location x_c^{des} at a specific time T and/or have a particular velocity \dot{x}_c^{des} at a given time t_v . To obtain the corresponding equations in the unknowns α_i , it is sufficient to rewrite the CoM position and velocity in terms of, for example, the initial CoM position $x_c(0)$

$$\begin{aligned}
 x_c^{\text{des}} &= \sum \alpha_i \{ z_{\text{step}}(T - t_i) + e^{-\omega_o t_i} \sinh(\omega_o T) \\
 &\quad - \cosh(\omega_o(T - t_i)) z_{\text{step}}(T - t_i) \} + e^{-\omega_o T} x_c(0) \\
 \dot{x}_c^{\text{des}} &= \omega_o \left[-e^{-\omega_o t_v} x_c(0) + \sum \alpha_i \{ e^{-\omega_o t_i} \cosh(\omega_o t_v) \right. \\
 &\quad \left. - \sinh(\omega_o(t_v - t_i)) z_{\text{step}}(t_v - t_i) \} \right]
 \end{aligned}$$

Note finally that these conditions are satisfied at a specific instant and need to be compatible with other design requirements.

VII. SIMULATION RESULTS

To validate the illustrated approach, the walking algorithm has been tested on the REEM-C robot in the Gazebo simulation environment. Gazebo is an open-source 3D simulator that includes an accurate simulation of rigid-body physics. REEM-C is a biped humanoid robot developed and commercialized by Pal Robotics as a research platform (Fig. 6).



Fig. 6. REEM-C biped robot platform

The robot is 1.65 meters tall, weights 80 kg and has 44 degrees of freedom: 6x2 in the legs, 2 in the waist, 2 in the head, 7x2 in the arms and 7x2 in the hands. The available sensors are absolute and relative joint encoders, 6 axis force/torque sensors in the ankles, IMU, 2 laser range finders, stereo cameras, microphones and speakers. Simulation runs at 1 KHz, while the walking algorithm is executed at 200 Hz. The walking solver computes the reference trajectories for the ZMP and CoM and an inverse kinematics algorithm is used for providing reference positions to joint PID controllers at every control cycle. A ZMP closed-loop controller is used to compensate for disturbances and differences between the simplified inverted pendulum model and the real system.

Preliminary experiments have been carried out in order to validate the ideas introduced in Section IV. The CoM has, for simplicity, been considered fixed with the humanoid's structure at a constant height of 0.7 m. In spite of this approximation, the use of the LIPM and very little tuning of the ZMP trajectory, these first results are very encouraging. In particular we report the CoM reference and actual trajectories in Fig. 7 together with the chosen reference ZMP. The CoM errors w.r.t. to the reference are shown in Fig. 8 where the initial errors are more evident. A reconstructed ZMP signal in the Gazebo environment is also shown in Fig. 10. To evaluate the contribution of the stabilizer, Fig. 9 shows the brute application of the reference CoM trajectory with no stabilizer. A short video of the REEM-C full simulation in Gazebo has been also included.

These preliminary results correspond to a desired ZMP trajectory with the single support represented by a constant value while the double support phase is a cubic polynomial. In the near future we plan to experiment the

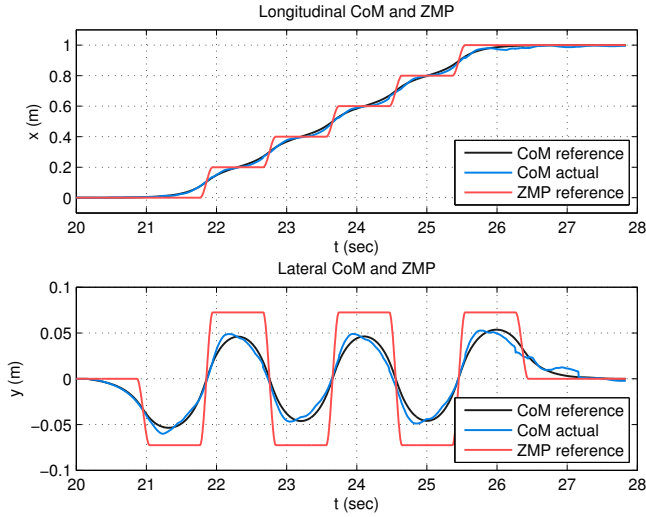


Fig. 7. CoM and ZMP trajectories

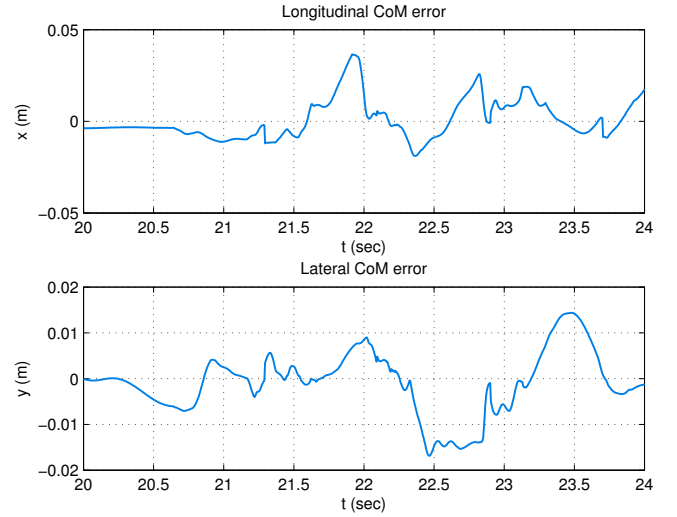


Fig. 9. CoM errors no stabilizer

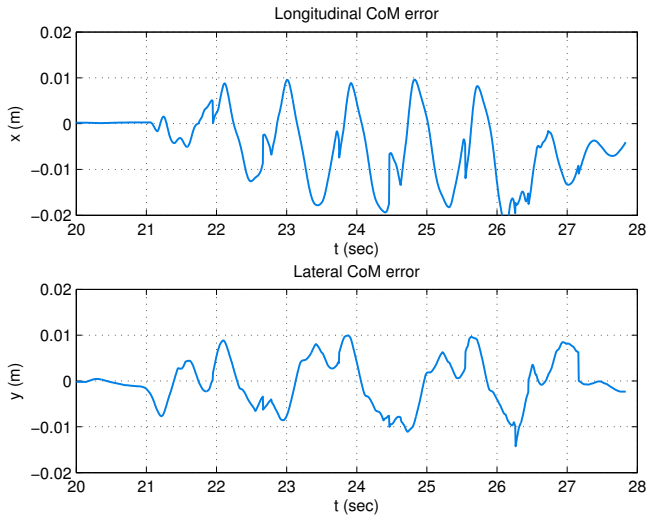


Fig. 8. CoM errors

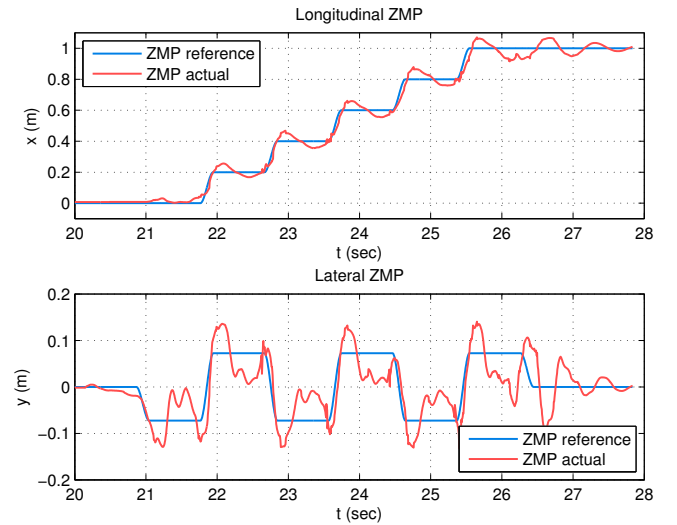


Fig. 10. ZMP reference vs actual

design approach illustrated in Section V-B by using this Constant/Cubic/Constant pattern as a basis function z_i .

VIII. DISCUSSION AND FUTURE WORK

A. Boundary Value Problems

It is important to stress the basic differences in the proposed approach w.r.t. to well-known results and these differences become clearer when referred to the corresponding Boundary Value Problem (BVP). Basically we have a linear second order differential equation driven by a fixed, for now, input. The generic solution needs two constraints to be uniquely defined. We may, at this stage, have basically three options:

- (A) The two constraints are defined by the initial and final position of the CoM (as in [3]). Note that the final CoM position condition can be restated as an initial velocity CoM constraint. Defining a final CoM position for the specific unstable z_i

at hand helps in limiting the diverging behavior associated with the particular solution.

- (B) Choosing as initial conditions $x_c^*(0; z)$ and $\dot{x}_c^*(0; z)$ we obtain a different solution with the characteristics previously discussed in Section IV.
- (C) A third option can be devised by imposing the boundedness constraint (14) and, for example, the initial CoM position $x_c(0)$ as shown in (V-A). The solutions of this third BVP are given by (17).

The three cases are summarized in Fig. 11.

B. Desired vs. Actual ZMP Trajectories

The three approaches described above define desired state trajectories for the CoM. It is important to stress that in all three cases, the actual initial conditions will rarely match the desired initial conditions. Therefore, some sort of feedback (stabilizer) is required, and the closed-loop dynamics of the resulting system will produce trajectories that match

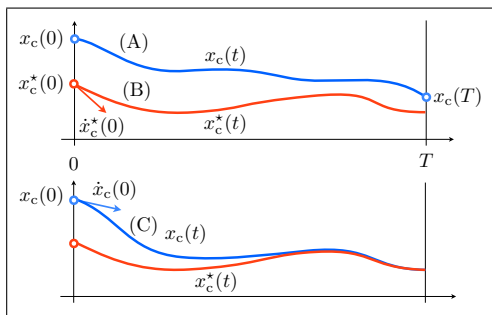


Fig. 11. Boundary value problems

the desired ones only asymptotically. Therefore, during the transient, the real ZMP will differ from the desired ZMP. An analysis of this error is possible in this framework.

C. Future Work

The approach that we have presented is amenable to real-time planning, and in the future we hope to investigate online implementations for planning and re-planning footsteps during gait execution. Moreover, following the ideas of [7], the family of ZMP trajectories can be enriched by including the effect of the swinging leg.

We also would like to investigate what appear to be close connections between our approach and the approach reported in [23].

Moreover, we will extend our approach to nonlinear systems, and specifically to derive boundedness conditions that can be directly applied to nonlinear models for biped locomotion.

Finally, we will continue to pursue real-world implementation and experimentation using the REEM-C robot.

IX. CONCLUSIONS

In this paper, we have presented an approach to trajectory planning for a bipedal robot. We began with a linearized approximation of the biped dynamics, and developed an explicit boundedness constraint on the relationship between the input and the initial conditions. For a sufficiently rich class of inputs, it is possible to satisfy the boundedness constraint while using remaining degrees of freedom to satisfy other performance goals. This idea formed the basis for our proposed trajectory planning method, which we illustrated for several typical problems. Finally, we have provided preliminary experimental validation of our approach using the REEM-C biped that has been developed by Pal Robotics.

REFERENCES

- [1] S. Kajita, T. Yamaura, and A. Kobayashi, "Dynamic walking control of a biped robot along a potential energy conserving orbit," *Robotics and Automation, IEEE Transactions on*, vol. 8, no. 4, pp. 431–438, Aug 1992.
- [2] S. Kajita, F. Kanehiro, K. Kaneko, K. Fujiwara, K. Harada, K. Yokoi, and H. Hirukawa, "Biped walking pattern generation by using preview control of zero-moment point," in *Robotics and Automation, 2003. Proceedings. ICRA '03. IEEE Int. Conference on*, vol. 2, 2003, pp. 1620–1626.
- [3] K. Harada, S. Kajita, K. Kaneko, and H. Hirukawa, "An analytical method on real-time gait planning for a humanoid robot," in *Humanoid Robots, 2004 4th IEEE/RAS Int. Conference on*, vol. 2, 2004, pp. 640–655.
- [4] K. Harada, K. Miura, M. Morisawa, K. Kaneko, S. Nakaoka, F. Kanehiro, T. Tsuji, and S. Kajita, "Toward human-like walking pattern generator," in *Intelligent Robots and Systems, 2009. IROS 2009. IEEE/RSJ Int. Conference on*, 2009, pp. 1071–1077.
- [5] K. Harada, S. Kajita, F. Kanehiro, K. Fujiwara, K. Kaneko, K. Yokoi, and H. Hirukawa, "Real-time planning of humanoid robot's gait for force-controlled manipulation," *Mechatronics, IEEE/ASME Transactions on*, vol. 12, no. 1, pp. 53–62, Feb 2007.
- [6] S. Kajita, M. Morisawa, K. Miura, S. Nakaoka, K. Harada, K. Kaneko, F. Kanehiro, and K. Yokoi, "Biped walking stabilization based on linear inverted pendulum tracking," in *Intelligent Robots and Systems (IROS), 2010 IEEE/RSJ Int. Conference on*, Oct 2010, pp. 4489–4496.
- [7] T. Takenaka, T. Matsumoto, and T. Yoshiike, "Real time motion generation and control for biped robot -1st report: Walking gait pattern generation-," in *Intelligent Robots and Systems, 2009. IROS 2009. IEEE/RSJ Int. Conference on*, 2009, pp. 1084–1091.
- [8] M. Morisawa, K. Harada, S. Kajita, K. Kaneko, F. Kanehiro, K. Fujiwara, S. Nakaoka, and H. Hirukawa, "A biped pattern generation allowing immediate modification of foot placement in real-time," in *Humanoid Robots, 2006 6th IEEE-RAS Int. Conference on*, Dec 2006, pp. 581–586.
- [9] T. Sugihara and Y. Nakamura, "Boundary condition relaxation method for stepwise pedipulation planning of biped robots," *Robotics, IEEE Transactions on*, vol. 25, no. 3, pp. 658–669, June 2009.
- [10] T. Buschmann, S. Lohmeier, M. Bachmayer, H. Ulbrich, and F. Pfeiffer, "A collocation method for real-time walking pattern generation," in *Humanoid Robots, 2007 7th IEEE-RAS Int. Conference on*, 2007, pp. 1–6.
- [11] P. B. Wieber, "Trajectory free linear model predictive control for stable walking in the presence of strong perturbations," in *Humanoid Robots, 2006 6th IEEE-RAS Int. Conference on*, 2006, pp. 137–142.
- [12] K. Erbaturo and O. Kurt, "Natural zmp trajectories for biped robot reference generation," *Industrial Electronics, IEEE Transactions on*, vol. 56, no. 3, pp. 835–845, 2009.
- [13] J. Pratt, J. Carff, S. Drakunov, and A. Goswami, "Capture point: A step toward humanoid push recovery," in *Humanoid Robots, 2006 6th IEEE-RAS Int. Conference on*, 2006, pp. 200–207.
- [14] B. Stephens, "Humanoid push recovery," in *Humanoid Robots, 2007 7th IEEE-RAS Int. Conference on*, 2007, pp. 589–595.
- [15] D. Wight, E. Kubica, and D. Wand, "Introduction of the foot placement estimator: A dynamic measure of balance for bipedal robotics," *J. of Computational and Nonlinear Dynamics*, vol. 3, pp. 1–9, 2007.
- [16] C. Santacruz and Y. Nakamura, "Reactive stepping strategies for bipedal walking based on neutral point and boundary condition optimization," in *Robotics and Automation (ICRA), 2013 IEEE Int. Conference on*, May 2013, pp. 3110–3115.
- [17] J. Engelsberger, C. Ott, and A. Albu-Schaffer, "Three-dimensional bipedal walking control using divergent component of motion," in *Intelligent Robots and Systems (IROS), 2013 IEEE/RSJ Int. Conference on*, Nov 2013, pp. 2600–2607.
- [18] T. Koolen, T. de Boer, J. Reubla, A. Goswami, and J. Pratt, "Capturability-based analysis and control of legged locomotion, part 1: Theory and application to three simple gait models," *The International Journal of Robotics Research*, vol. 31, no. 9, pp. 1094–1113, 2012.
- [19] M. Vukobratovic and D. Juricic, "Contribution to the synthesis of biped gait," *Biomedical Engineering, IEEE Transactions on*, vol. BME-16, no. 1, pp. 1–6, 1969.
- [20] A. Hof, M. Gazendam, and W. Sinke, "The condition for dynamic stability," *Journal of Biomechanics*, vol. 38, no. 1, pp. 1–8, 2005.
- [21] L. Lanari and J. Wen, "Feedforward calculation in tracking control of flexible robots," in *Decision and Control, 1991., Proceedings of the 30th IEEE Int. Conference on*, vol. 2, 1991, pp. 1403–1408.
- [22] S. Devasia and B. Paden, "Exact output tracking for nonlinear time-varying systems," in *Decision and Control, 1994., Proceedings of the 33rd IEEE Conference on*, vol. 3, 1994, pp. 2346–2355.
- [23] J. Urata, K. Nshiwaki, Y. Nakanishi, K. Okada, S. Kagami, and M. Inaba, "Online decision of foot placement using singular lq preview regulation," in *Humanoid Robots (Humanoids), 2011 11th IEEE-RAS Int. Conference on*, Oct 2011, pp. 13–18.